ACCOUNTS of chemical research

Article

pubs.acs.org/accounts

Flow-Directed Crystallization for Printed Electronics

Ge Qu,[†,§] Justin J. Kwok,[‡,§] and Ying Diao*[,†]

[†]Department of Chemical & Biomolecular Engineering, University of Illinois at Urbana−Champaign, 600 South Mathews Avenue, Urbana, Illinois 61801, United States

[‡]Department of Materials Science and Engineering, University of Illinois at Urbana−Champaign, 1304 W. Green St., Urbana, Illinois 61801, United States

CONSPECTUS: The solution printability of organic semiconductors (OSCs) represents a distinct advantage for materials processing, enabling low-cost, high-throughput, and energy-efficient manufacturing with new form factors that are flexible, stretchable, and transparent. While the electronic performance of OSCs is not comparable to that of crystalline silicon, the solution processability of OSCs allows them to complement silicon by tackling challenging aspects for conventional photolithography, such as large-area electronics manufacturing. Despite this, controlling the highly non-equilibrium morphology evolution during OSC printing remains a challenge, hindering the achievement of high electronic device performance and the elucidation of structure−property relationships. Many elegant morphological control methodologies have been developed in recent years including molecular design and novel processing approaches, but few have utilized fluid flow to control morphology in OSC thin films. In this Account, we discuss flow-directed crystallization as an effective strategy for controlling the crystallization kinetics during printing of small molecule and polymer semiconductors. Introducing the concept of flow-directed crystallization to the field of printed electronics is inspired by recent advances in pharmaceutical manufacturing and flow processing of flexible-chain polymers. Although flow-induced crystallization is well studied in these areas, previous findings may not apply directly to the field of printed electronics where the molecular structures (i.e., rigid π-conjugated backbone decorated with flexible side chains) and the intermolecular interactions (i.e., $\pi-\pi$ interactions, quadrupole interactions) of OSCs differ substantially from those of pharmaceuticals or flexible-chain polymers. Another critical difference is the important role of solvent evaporation in open systems, which defines the flow characteristics and determines the crystallization kinetics and pathways. In other words, flow-induced crystallization is intimately coupled with the mass transport processes driven by solvent evaporation during printing. In this Account, we will highlight these distinctions of flow-directed crystallization for printed electronics.

In the context of solution printing of OSCs, the key issue that flow-directed crystallization addresses is the kinetics mismatch between crystallization and various transport processes during printing. We show that engineering fluid flows can tune the kinetics of OSC crystallization by expediting the nucleation and crystal growth processes, significantly enhancing thin film morphology and device performance. For small molecule semiconductors, nucleation can be enhanced and patterned by directing the evaporative flux via contact line engineering, and defective crystal growth can be alleviated by enhancing mass transport to yield significantly improved coherence length and reduced grain boundaries. For conjugated polymers, extensional and shear flow can expedite nucleation through flow-induced conformation change, facilitating the control of microphase separation, degree of crystallinity, domain alignment, and percolation. Although the nascent concept of flow-directed solution printing has not yet been widely adopted in the field of printed electronics, we anticipate that it can serve as a platform technology in the near future for improving device performance and for systematically tuning thin film morphology to construct structure−property relationships. From a fundamental perspective, it is imperative to develop a better understanding of the effects of fluid flow and mass transport on OSC crystallization as these processes are ubiquitous across all solution processing techniques and can critically impact charge transport properties.

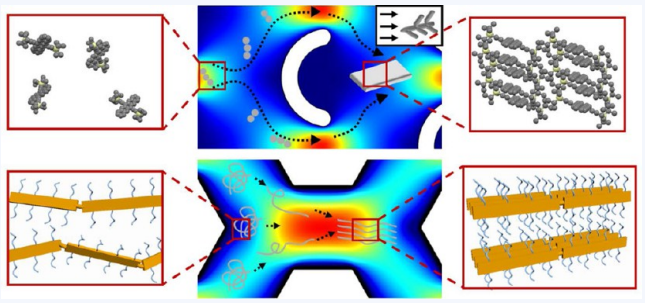

1. INTRODUCTION

Over the past 30 years, organic semiconductors (OSCs) have emerged as a new class of electronic and optoelectronic materials that are intrinsically lightweight and flexible and can be processed using energy-efficient, high-throughput methods such as solution printing. Organic semiconductors have demonstrated potential uses in a diverse range of applications including transistors,[1] thermoelectrics,[2] sensors,[3], light-emitting diodes[4] and solar cells.[5] Thanks to rapid materials innovations, the last 30 years have witnessed over a 6 orders of magnitude improvement in charge carrier mobilities for organic semiconductors, pointing toward a bright future for organic electronics.[6]

Received: August 31, 2016
Published: November 29, 2016

DOI: 10.1021/acs.accounts.6b00445
Acc. Chem. Res. 2016, 49, 2756−2764

Compatibility with energy-efficient, high-throughput solution printing methods represents a significant advantage of solution printable organic semiconductors compared with traditional semiconductors. The solution printability at near ambient conditions also enables deposition on polymer substrates to implement flexible, stretchable, and wearable form factors. On the other hand, key challenges remain: how does molecular assembly proceed during solution printing and how can the resulting thin film morphology be controlled? The significance of these challenges lies in the fact that charge transport in printed thin films is highly sensitive to their morphological parameters across all length scales.[6] These parameters include intramolecular conformation (torsion angle) and intermolecular ordering ($\pi-\pi$ stacking, paracrystallinity) at the molecular scale,[7−13] crystallite size and domain percolation at the mesoscale,[14] and domain alignment and boundary distribution at the macroscale.[15] For further discussions on this topic, we refer the readers to these excellent reviews on morphology−charge transport relationship for organic field-effect transistor applications.[6,12,16]

Many methods have been developed to control thin film morphology via either molecular design or novel processing techniques.[17,18] Recently reported processing methods include additive, UV light or ultrasound induced crystallization,[14,19−21] templating,[22−24] evaporation control,[25−27] and unidirectional coating.[28−30] Even so, the fluid dynamics and transport aspects influencing the molecular assembly of OSCs have been largely neglected in the literature. During solution printing, the molecular assembly process is tightly coupled with the complex transport processes, which include mass transport of solute via convection and diffusion in the solution, mass transport of solvent through evaporation, and heat transfer within and across phase boundaries. As a result, multiple time scales exist, the competition among which determines the final morphology of the printed films. A significant hurdle in high-throughput solution printing is the time scale mismatch between coupled processes, which frequently results in nonideal morphology. For instance, dendritic growth of small molecules arises from a time scale mismatch between crystal growth and solute diffusion and vitrification of polymers is attributed to a time scale mismatch between polymer nucleation and solvent evaporation. Designing fluid flow provides the opportunity to tune the crystallization and transport processes in order to match time scales, thereby serving as an effective morphological control method that is directly transferrable to large-scale solution printing. In industrial-scale solution printing, such as roll-to-roll printing processes, methods of controlling fluid flow may be incorporated into OSC fabrication since engineered flows have been successfully demonstrated in these scalable processes in lab-scale experiments.[31] Some excellent review papers provide comprehensive discussions on OSC solution printing methods and potential large scale applications if further discussion is needed.[32,33]

2. FLOW-DIRECTED SMALL MOLECULE CRYSTALLIZATION

2.1. Mass-Transport Directed Nucleation

While fluid flow has only recently been explored as a means to enhance crystallization of organic semiconductors, this method is well-known in other fields, such as pharmaceuticals and the food industry wherein the flow effect has been studied in enclosed crystallizers. Early works by Mullin and Raven

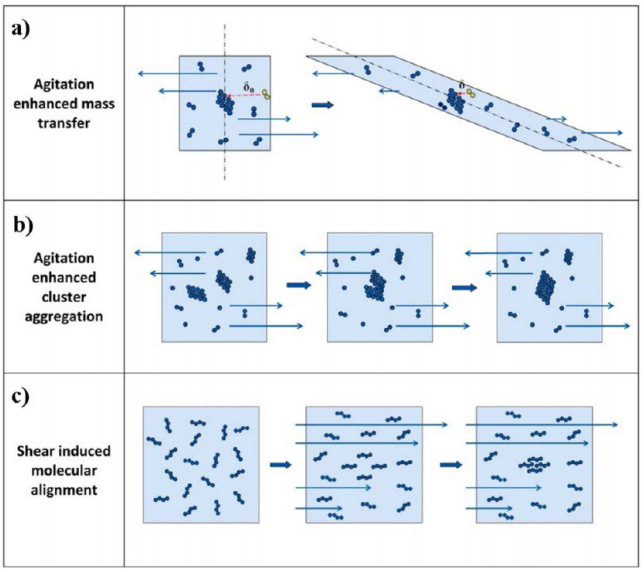

Figure 1. Schematic representations of fluid flow effects on small molecules. (a) Enhanced mass transport, (b) cluster coalescence, and (c) molecular alignment. Reproduced with permission from ref 36. Copyright 2016 American Chemical Society.

suggested that fluid agitation enhances mass transport and thereby increases the nucleation rates (Figure 1a).[34,35] Recent works studying the effects of fluid flow on induction time have also observed increased kinetics but suggest that the underlying mechanism is instead most likely cluster coalescence (Figure 1b),[36] where the collision of prenuclei clusters results in coalescence and the expedited formation of larger clusters. A third mechanism is the alignment of molecules along the direction of flow due to shear (Figure 1c).

In solution printing, the crystallization environment and transport processes are drastically different from those inside an enclosed crystallizer. In the case of meniscus-guided solution printing, convective flow arises from solvent evaporation as well as from the viscous forces imposed by the substrate.[37] The contribution from solvent evaporation is also known as capillary flow, same as observed in the coffee ring effect.[38] It has been shown that the evaporative flux is the greatest at the droplet contact line, resulting in an outward, accelerating flow near the solid−liquid interface (Figure 2b,d). Regions of the contact line with high convex curvature or high surface area to volume ratio correspond to higher evaporative fluxes and stronger fluid flows causing particles within the droplet to aggregate the fastest in these regions. Capillary flow also occurs due to evaporation at the meniscus front during solution printing, leading to solute deposition (Figure 2a). This has been utilized in many studies to induce alignment of crystalline domains along the coating direction, often with the fastest growth axis of organic semiconductor crystals aligned with the coating direction.[7,17,30]

In solution printing, however, convective flow also arises from viscous forces imposed by the substrate or blade during coating. In such cases, there are in fact two regimes, the evaporation regime and the Landau−Levich regime,[37] which can alter the deposition mechanism and the film thickness. In the evaporation regime, the coating speed is sufficiently low that the convective flow is dominated by evaporation-driven capillary flow, resembling the coffee-ring effect. The evaporation induces solute supersaturation at the meniscus, resulting in nucleation at the contact line and causing the crystal growth

DOI: 10.1021/acs.accounts.6b00445
Acc. Chem. Res. 2016, 49, 2756−2764

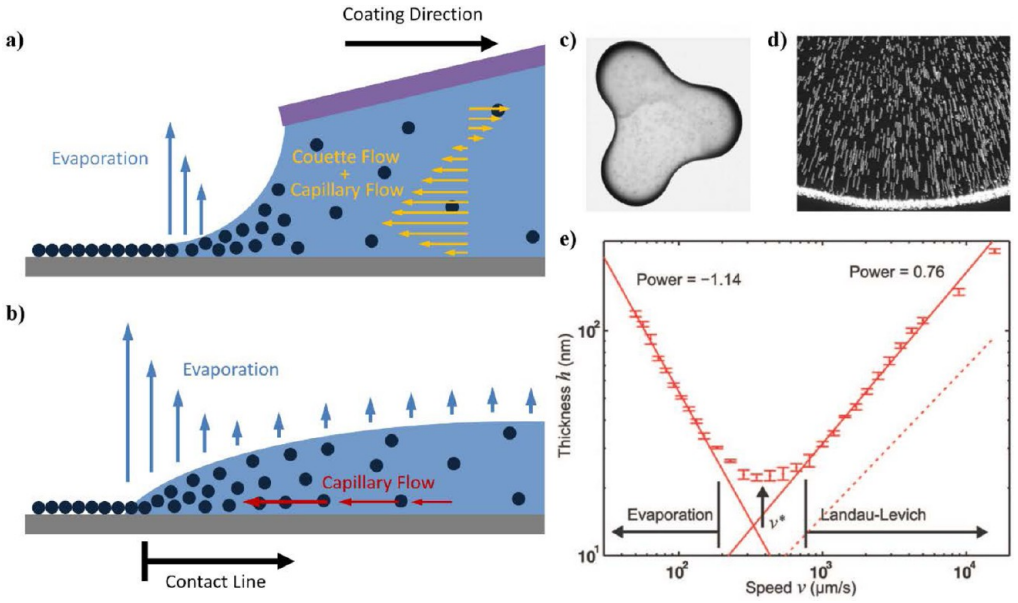

Figure 2. Transport processes in an evaporating meniscus. (a) Schematic of unidirectional coating driven by evaporation. (b) Schematic of a droplet undergoing the coffee ring effect. (c) Image of droplet with regions of high curvature. (d) Convective flow of particles toward the contact line. Reproduced with permission from ref 38. Copyright 1997 Nature Publishing Group. (e) The evaporation and Landau−Levich regimes observed during the blade coating of a phospholipid solution onto a silicon substrate at 27 °C. The phospholipid solution consisted of 98 wt % DOPC and 2 wt % NBD-PC dissolved in *n*-octane at 20 mg/mL. Reproduced with permission from ref 37. Copyright 2009 American Chemical Society.

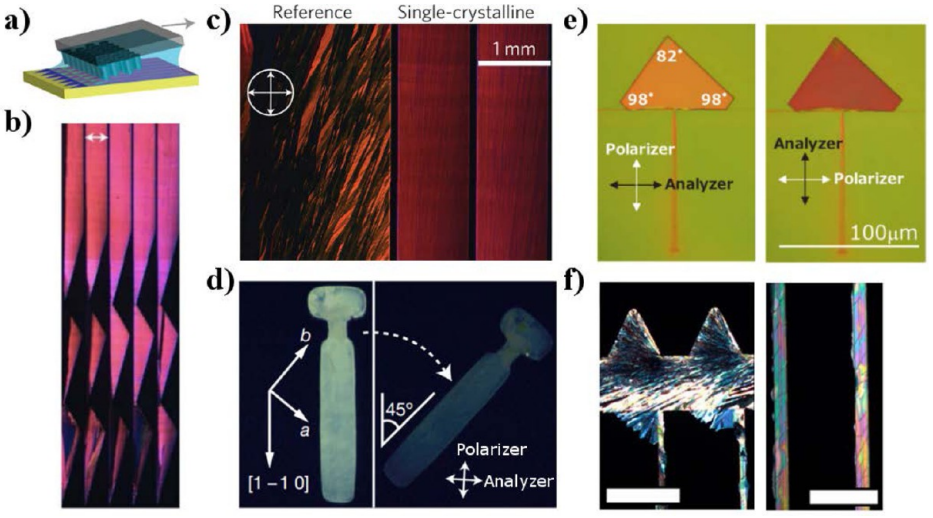

Figure 3. Nucleation control by tuning solvent evaporation. (a) Schematic of the FLUENCE coating scheme. (b) Control of nucleation and selection of growth direction using triangular wetting zones (strips 500 μm wide as indicated by arrow). (c) CPOM of film produced with FLUENCE (right) and without (left). Reproduced with permission from ref 9. Copyright 2013 Nature Publishing Group. (d) CPOM of a singular C8-BTBT crystal formed from an asymmetric pattern. Reproduced with permission from ref 25. Copyright 2011 Nature Publishing Group. (e) Nucleation of C2Ph-PXX in a thin region followed by single crystal growth into the large region. Reproduced with permission from ref 26. Copyright 2012 Wiley. (f) Nucleation on triangular thiophenol-functionalized Au regions (left) followed growth toward the leading electrodes (right) (scale bar 100 μm). Reproduced with permission from ref 40. Copyright 2015 National Academy of Sciences.

velocity to match that of the receding meniscus. By applying a simple mass balance, it was derived that the film thickness scales with the inverse of the coating speed v^{-1} (Figure 2e). As coating speed increases into the Landau−Levich regime, the convective flow becomes dominated by the viscous force. In other words, the amount of solvent dragged out by the viscous force is larger than the amount of solvent evaporated. In this regime, the liquid film drag-out is followed by uniform solvent evaporation, initiating sporadic nucleation across the entire liquid film. The film thickness is determined by substrate-imposed viscous shear stress counterbalancing the front meniscus surface stress and the back meniscus capillary pressure, scaling with $v^{2/3}$ (Figure 2e).[37] Equating the two models gives the critical coating speed at which the regime transitions, as seen in Figure 2e, first proposed by Le Berre and colleagues.[37] As expected, the morphology of the resulting films can vary greatly due to the difference in deposition mechanism. In Giri et al.,[39] low coating speeds of ≤2.8 mm/s produced films with TIPS−pentacene domains aligned with the coating direction. At 4 mm/s, a comet-shaped, transcrystalline

DOI: 10.1021/acs.accounts.6b00445
Acc. Chem. Res. 2016, 49, 2756−2764

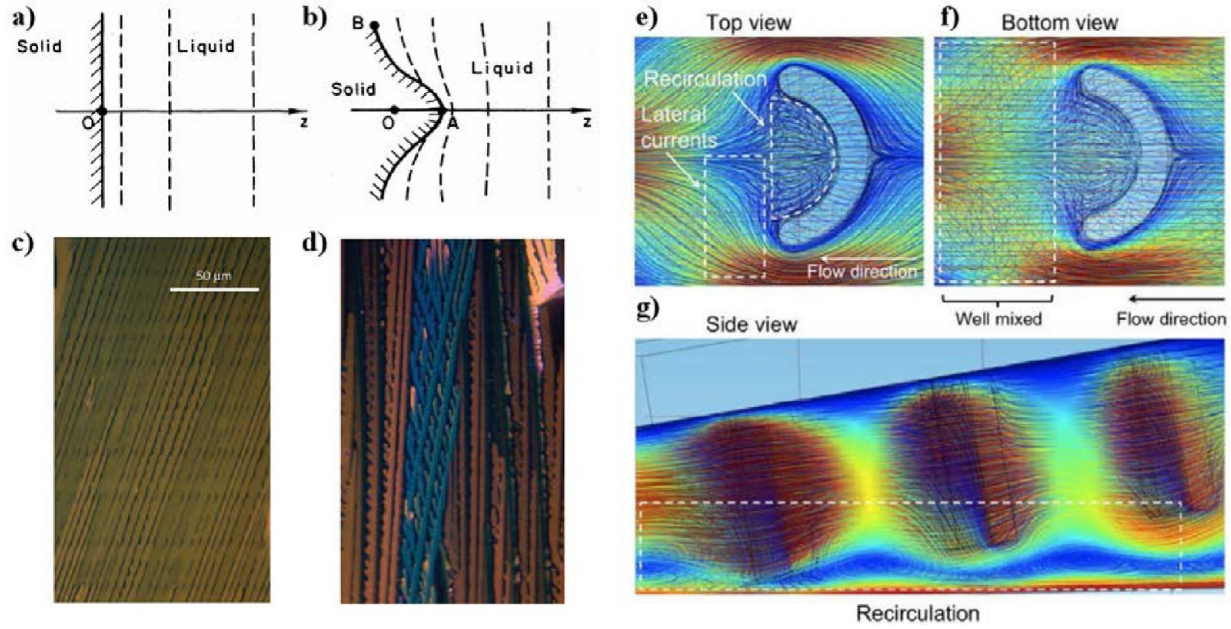

Figure 4. Depiction of Mullins–Sekerka instability. (a) Flat interface with uniform concentration gradient. (b) Protrusion at the interface steepening the concentration gradient surrounding it. Reproduced with permission from ref 44. Copyright 1980 American Physical Society. TIPS-pentacene film produced (c) with micropillars and (d) without resulting in dendritic growth. Enhanced lateral mass transport as a result of flow separation around micropillars and recirculation behind micropillars, as determined from COMSOL simulations (e–g). Reproduced with permission from ref 9. Copyright 2013 Nature Publishing Group.

morphology was attained, and at 8 mm/s, a completely isotropic spherulitic film was produced.

Taking inspiration from the coffee ring effect, we have developed an approach to achieve nucleation control by designing the meniscus curvature to modulate the local evaporation rate.[9] The coating scheme, termed FLUENCE (fluid-enhanced crystal engineering) is shown in Figure 3a with resulting printed films in Figure 3b,c. It consists of a blade patterned with micropillars that spreads the ink solution across a temperature-controlled substrate with patterned wetting and dewetting zones. The purpose of introducing the micropillars is to induce lateral mass transport for enhancing crystal growth and will be discussed later. To control nucleation, the silicon substrate was patterned with phenyltrichlorosilane and octadecyltrichlorosilane for solvent wetting and dewetting zones, respectively. At the initial region, triangular wetting zones were patterned to induce high evaporative fluxes at the sharp corners by taking advantage of the high curvature (Figure 3b). The resulting capillary flow induces a higher concentration buildup toward the triangle tip aiding nucleation. Further triangular zones connected by small necks eliminate growth in unwanted directions. What follows are long strips of wetting surface where highly aligned single-crystalline domains grow (Figure 3c). Similar techniques for controlled nucleation have been demonstrated by Minemawari et al. and Goto et al. as shown in Figure 3d,e, respectively.[25,26] In both works, surface patterning of wetting zones was utilized to induce nucleation in areas with higher evaporation rates. More recently Park et al. have utilized nucleation control to produce transistor arrays with high yield and low variability using a method for controlled OSC nucleation and extension for circuits, termed CONNECT.[40] This was achieved by rendering Au source and drain electrodes wetting and the remaining SiO_2 surface dewetting. Nucleation first occurred on the sharp corners of the triangular Au regions before being directed to bridge the gaps between the trailing source–drain electrodes. Narrow gaps (0.5–20 μm) were designed to facilitate bridging of the OSC between the electrodes (Figure 3f). Using this method, researchers were able to achieve transistors with 99% yield and 28% relative variance in mobility, showing good uniformity.

2.2. Flow-Enhanced Crystal Growth

In meniscus-guided printing methods, where crystallization takes place in an open system, convection is induced due to the evaporation of solvent (i.e., capillary flow) as well as the viscous forces imparted by the blade or substrate (i.e., Couette flow). The presence of directional convective flow enhances crystal growth and causes alignment of the fastest growth axis with the coating direction when the time scale of crystal growth matches with the time scale of evaporation. Despite such an enhancement, mass transport transverse to the coating direction remains diffusive. At sufficiently high printing speeds, a time scale mismatch between slow solute transport and fast crystal growth leads to dendritic growth that induces undesired secondary nucleation and grain boundary formation. Dendritic structures contain low packing density and give rise to large amounts of defects, making it undesirable for charge transport. The mechanism for this type of growth was first studied in detail by Mullins and Sekerka.[41,42] A simple model that provides a qualitative description for crystal growth in solution is the diffusion-reaction model, which is characterized by the transport of solute to the crystal surface followed by a "surface reaction" describing the incorporation of the solute molecules into the crystal lattice.[43] Considering this model for crystal growth, when in the diffusion-limited regime, perturbations at the crystal–solution interface can grow larger as protrusions of the solid sharpen the concentration gradient surrounding it (Figure 4a,b) causing an instability.[44] When the "surface reaction" is the rate-limiting step, or in other words the growth is kinetic-limited, this Mullins–Sekerka instability no longer occurs. These two processes can be compared using a

DOI: 10.1021/acs.accounts.6b00445
Acc. Chem. Res. 2016, 49, 2756–2764

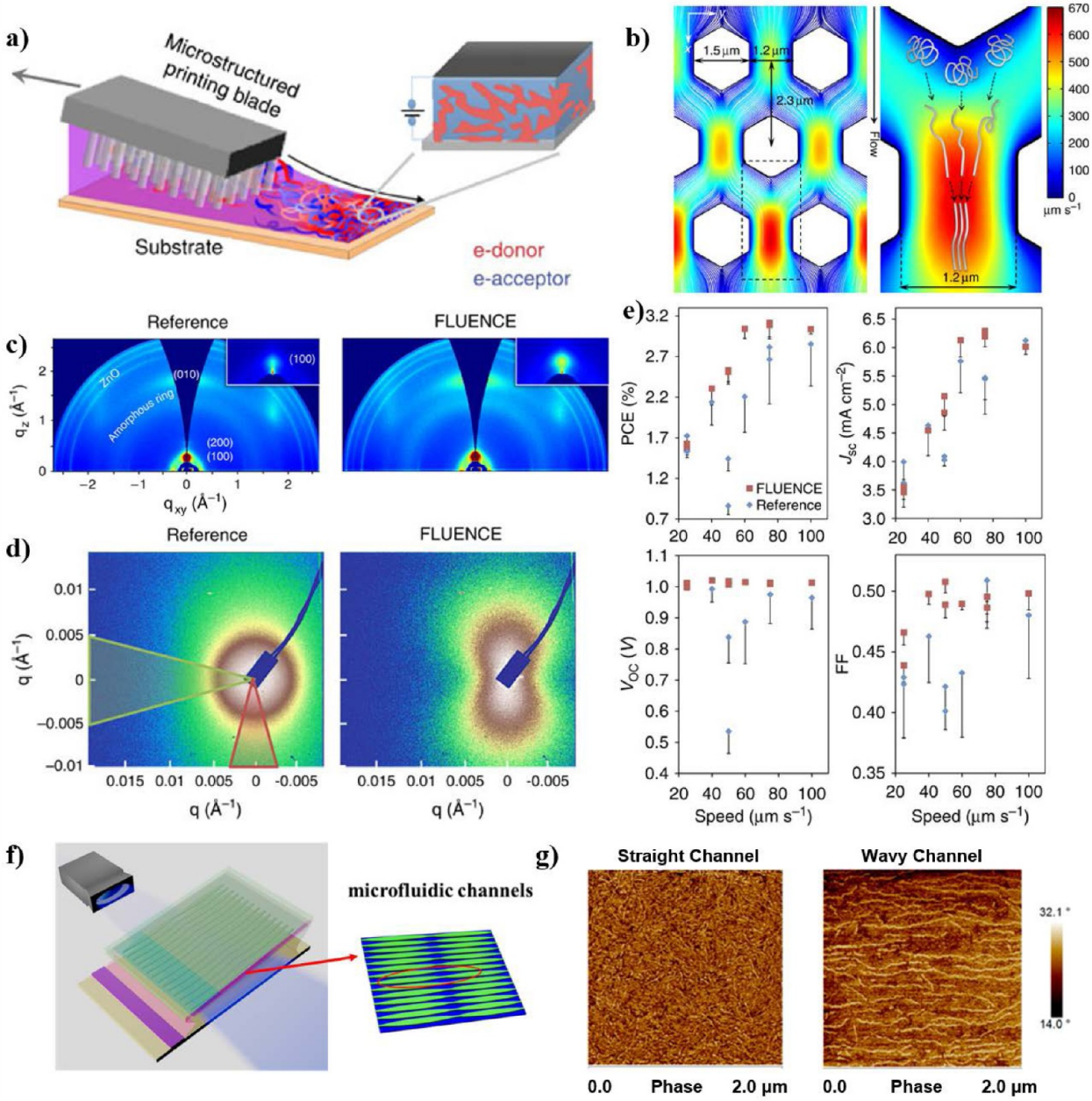

Figure 5. Extensional-flow-induced polymer nucleation. (a) Schematic of the FLUENCE method for printing bulk heterojunction solar cells. (b) Simulated flow field in FLUENCE printing, and the hypothetical flow-induced polymer conformation change. (c) GIWAXS images of neat donor polymer films printed without vs with the application of FLUENCE. (d) RSoXS images of the reference film vs FLUENCE-printed film at low printing speeds (<50 μm/s). (e) Solar cell device performance comparison between reference and FLUENCE-printed films. The figures shown are power conversion efficiency (PCE) and short-circuit current (J_{sc}) (top), and open circuit voltage (V_{oc}) and fill factor (FF) (bottom). Reproduced with permission from ref 5. Copyright 2015 Nature Publishing Group. (f) Schematic of solution coating with wave patterned blade and in situ UV-irradiation (wBPD-UV). (g) Tapping mode AFM phase image of P3HT film coated with straight channel blade and wave channel blade from UV incorporated solution printing. Reproduced with permission from ref 52. Copyright 2016 American Chemical Society.

dimensionless Damköhler number, $Da = kL/D$, where the rate constant k describes the surface kinetics, L is the characteristic length, and D is the diffusion coefficient, which describes diffusive mass transport. For $Da \gg 1$, crystal growth is diffusion-limited, and for $Da \ll 1$ crystal growth is kinetic-limited. When convection is present, the Péclet number, $Pe = UL/D$, where U is the fluid velocity, should also be considered as the ratio Da/Pe compares the surface reaction rate to the convection rate. Simulations have shown an increase in dendritic growth with increasing Da.[45] Therefore, providing sufficient mass transport can inhibit dendritic growth and improve morphology. To achieve this, we patterned the coating blade with crescent-shaped micropillars that arch against fluid flow.[9] There are several consequences of this design informed by fluid dynamic simulations, which encourage lateral convective mass transport, demonstrated in Figure 4e,f,g. First, the arch structure enhances flow separation, which induces a lateral component to the flow. Second, the narrow spacing between micropillars forces the flow to compress and expand as it exits. Third, the concave portion of the micropillar

DOI: 10.1021/acs.accounts.6b00445
Acc. Chem. Res. 2016, 49, 2756−2764

arches induces recirculation to further enhance lateral mass transport. The use of micropillars resulted in films containing much larger domains, significantly reduced defects, and no dendritic growth (Figure 4c,d). The in-plane X-ray coherence length for the printed films improved significantly with the use of micropillars for directions both parallel and perpendicular to the coating direction. OFETs fabricated using FLUENCE exhibited an average mobility of 8.1 ± 1.2 $cm^2\ V^{-1}\ s^{-1}$ with a relative variance of 14.7% while those printed without had an average mobility of 2.3 ± 0.7 $cm^2\ V^{-1}\ s^{-1}$ with a relative variance of 30.5% demonstrating the effectiveness of FLUENCE.

In recent work by Wang et al. similar principles of flow design were employed to produce 2,7-dioctyl[1]benzothieno-[3,2-*b*][1]benzothiophene (C8-BTBT) films for OFETs.[46] Researchers repurposed a commercially available rollerball pen to dispense C8-BTBT/anisole ink onto a hexamethyldisilazane-modified Si/SiO_2 surface. Using the rollerball pen, they were able to write crystalline films that were 500 μm wide with grain sizes reaching to several hundreds of micrometers. Fluid dynamics simulation results showed that the rollerball pen design induced lateral mass transport as a result of flow expansion through the gap between the ball and the refill tube. The increase in C8-BTBT domain size was attributed to the enhanced lateral mass transport.

3. FLOW-INDUCED POLYMER CRYSTALLIZATION

Macromolecules exhibit significant differences regarding the crystallization pathways and the resulting crystal morphology as compared to the case for small molecules.[47] The nucleation and growth of polymer crystals can occur through either chain folding or the aggregation of extended parallel chains. Under quiescent conditions, typically the time necessary to achieve fully extended parallel chains is much longer than the time to form chain folded lamellar structures, especially for longer polymer chains.[47] The time scales for conformation change are influenced by several intrinsic factors including the backbone rigidity and the molecular weight. For semiconducting polymers, the π-conjugation yields significantly higher backbone rigidity compared to aliphatic polymers. Miura et al. performed molecular dynamic simulations on melt crystallization of short polymer chains with various degrees of rigidity.[48] It was found that higher rigidity leads to higher crystalline order and shorter nucleation induction time since more rigid chains could stretch and grow together at the same time while more flexible chains must first stretch before being able to orient and associate together. Other aspects such as chain length, intermolecular interactions, and the surface energies of amorphous and crystalline regions can also influence the crystallization process. While such factors significantly impact crystallization, they are inherent material properties, which are difficult to tune or undesirable to alter. On the other hand, extrinsic factors such as flow fields have been extensively studied and applied for controlling crystallization of flexible chain polymers.[49]

Under the influence of flow, polymer chains can exhibit chain extension via the "coil-to-stretch" transition to aid nucleation and growth. Extensional flows have been found to be the most effective at extending polymer chains, although simple shear can also induce chain extension in polymer melts and concentrated solutions when chain entanglements occur.[49,50] In extensional flows, the frictional force of the surrounding fluid acting on a polymer coil is what induces the coil-to-stretch transition. The critical strain rate for inducing this transition can be predicted by the Weissenberg number, *Wi*, which is the product of the extensional strain rate $\dot{\varepsilon}$ and the longest polymer relaxation time τ. For $Wi > 1/2$, polymer chains are predicted to undergo the coil-to-stretch transition. Although flow-induced polymer crystallization has been extensively studied since the 1960s,[51] these studies have almost entirely focused on flexible-chain polymers. Understanding and application of flow-induced crystallization of rigid, conjugated polymers can open up new avenues for manufacturing high performance organic electronics and facilitate the much needed structure−property relationship studies by systematic tuning of thin film morphology.

3.1. Extensional-Flow-Induced Polymer Nucleation

In the context of printed electronics, the time scale mismatch between the sluggish polymer nucleation and rapid solvent evaporation often results in nonideal thin film morphology and device performance. Our recent work demonstrates that introducing extensional flow during solution printing can serve as an effective strategy for enhancing nucleation, thereby addressing the kinetics mismatch. We demonstrated this concept for printing all-polymer solar cells.[5] One challenge in this area lies in the large-scale microphase separation resulting in domains larger than the exciton diffusion length that hinder efficient charge generation at the donor−acceptor interface. Our strategy was to reduce domain size by increasing polymer nucleation density via extensional-flow-induced nucleation. Our method serves as an alternative to the widely employed solvent additive method for tuning domain sizes.[19,20]

Meniscus-guided solution printing is dominated by shear flow due to no slip boundary conditions, accompanied by weak extension from the accelerating capillary flow (Figure 2a). To enhance extensional flow, we applied the FLUENCE method that we originally developed for printing highly aligned small molecule single crystals, patterning the printing blade with tightly packed hexagonal micropillar arrays (Figure 5a). Using micropillar arrays, the maximum extensional strain rate increased by ∼2 order of magnitude to ∼500 s^{-1} (Figure 5b). As a result, polymer nucleation was promoted as evidenced by the enhanced degree of crystallinity probed by grazing incidence wide-angle X-ray diffraction (GIWAXS) (Figure 5c) and the reduced domain size measured by resonant soft X-ray scattering (RSoXS) (Figure 5d). Reduced domain sizes and improved molecular ordering enhanced the solar cell performance by all metrics (Figure 5e). The small pillar spacing in this design is critical for inducing high extensional strain rates that correspond to a high Weissenberg number for chain stretching. We found that the effect of enhanced nucleation diminished when the spacing of the micropillars increased from 1.2 to 15 μm, reducing the maximum extensional strain rate by ∼170 times. To further establish quantitative design principles, measurements of polymer relaxation time and crystallization kinetics are still needed. Recently Wang et al. also implemented structured blade design to induce extensional flow during solution printing with UV irradiation, resulting in crystallinity and morphology enhancement in printed P3HT thin films.[52] The coating blade was patterned with wave-like structures with compression and expansion regimes (Figure 5f), where extensional flow arises from the change in fluid velocity within the channels. Improved film morphology with long, aligned fibers was revealed by AFM on the films printed using the wavy channel blade, while randomly oriented short fibers appeared

DOI: 10.1021/acs.accounts.6b00445
Acc. Chem. Res. 2016, 49, 2756−2764

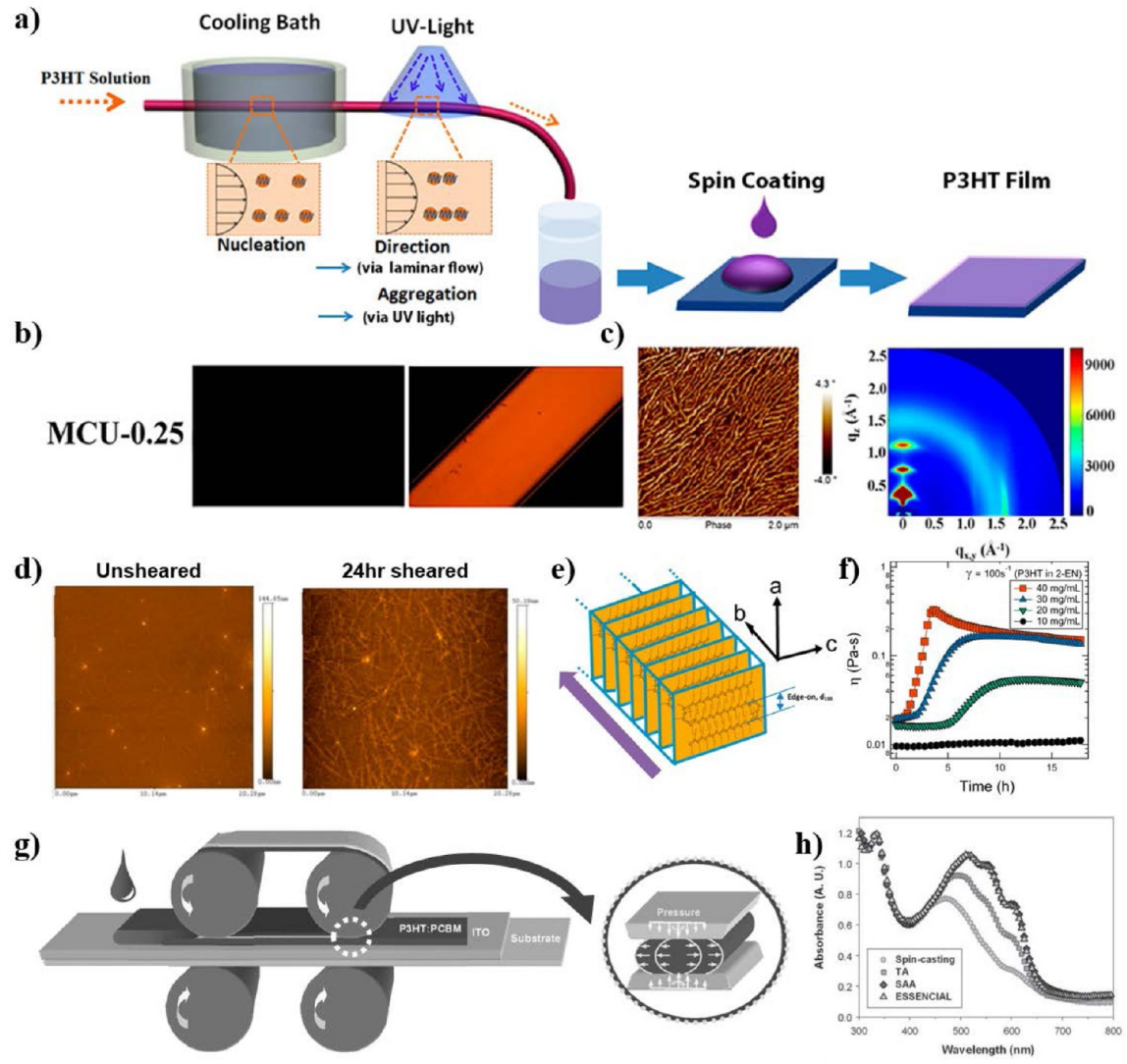

Figure 6. Shear-induced polymer nucleation. (a) Schematic of MCU (microfluidics cooling-UV) method followed by spin coating. (b) Cross-polarized microscopy image of P3HT/chloroform solution at the flow rate of 0.25 m/s. (c) Tapping mode AFM phase image and GIWAXS image of P3HT thin films on Si substrate at the optimum condition, MCU-0.25. Reproduced with permission from ref 21. Copyright 2015 American Chemical Society. (d) Tapping mode AFM image of films spin coated from P3HT/2-ethylnaphthalene solution at 10 mg/mL under unsheared and 24 h sheared conditions. (e) Schematic of molecular stacking in P3HT fibrils. The arrow indicates the fibril long axis. (f) Change in viscosity over time under a steady shear rate of P3HT solution at various concentrations. Reproduced with permission from ref 53. Copyright 2014 American Chemical Society. (g) Schematic of roll-to-roll coating with shear denoted as ESSENCIAL. (h) UV−vis spectra of thin film solar cell deposited from multiple methods. Reproduced with permission from ref 31. Copyright 2010 Wiley.

on the films printed using the straight channel blade (Figure 5g). The contrast in film morphology proved the effectiveness of extensional flow for inducing crystallization compared to shear flow alone.

3.2. Shear-Induced Polymer Nucleation

Besides extensional flow, shear flow has been employed to promote conjugated polymer nucleation, using P3HT as the model system.[21,31,53] In a study by Wang et al.,[21] a tubular flow of P3HT in chloroform solution was subjected to cooling and UV treatments before being spin-coated into thin films (Figure 6a). Introducing shear flow together with cooling and UV irradiation significantly enhanced P3HT solution aggregation and alignment (Figure 6b). In the subsequent spin-coated films, the P3HT fiber length increased and the crystallinity was significantly improved as revealed by AFM and GIXD, respectively (Figure 6c). In the absence of UV irradiation and with cooling alone the effect of shear flow was diminished. The synergistic effect of UV and shear flow is unclear. In another study, Wie et al. applied a continuous shear for over 24 h to P3HT dissolved in 2-ethylnaphthalene to find a strongly concentration dependent shear effect on crystallization kinetics as measured by viscosity change (Figure 6d−f).[53] A much more significant viscosity change under shear was observed when the polymer concentration was increased beyond the percolation threshold (Figure 6f). The authors proposed that shear flow promotes conformational change of the polymer chains brought together by Brownian motion, thereby inducing crystallization. In a P3HT/PCBM blend solution system, Park et al. fabricated thin film solar cells in a roll-to-roll printing setup where shear stress was applied to the liquid film. The process was named ESSENCIAL (Figure 6g).[31] Superior crystallinity was observed in ESSENCIAL films compared to

DOI: 10.1021/acs.accounts.6b00445
Acc. Chem. Res. 2016, 49, 2756−2764

those prepared using other deposition methods, judged from the higher absorption and more pronounced vibronic shoulders of the ESSENCIAL films analyzed by UV−vis spectroscopy (Figure 6h). The authors attributed the high crystallinity and solar cell performance to the effect of shear flow in roll-to-roll printing.

4. SUMMARY AND OUTLOOK

The precise control of thin film morphology is of great interest in the field of printed electronics for both understanding the charge transport mechanisms and attaining high device performance. The highly nonequilibrium molecular assembly process during solution printing poses significant challenges and at the same time offers unexplored opportunities for attaining high levels of morphological control. Under this backdrop, we, together with other groups in the field, demonstrate that designing printing flow is an emerging strategy for effectively controlling the crystallization process of both conjugated small molecule and polymer systems. On the other hand, many challenges remain in terms of both fundamental understandings and technological development of flow-induced crystallization of organic semiconductors. One fundamental challenge is the understanding of flow-induced crystallization in evaporative, open systems, where crystallization is intimately coupled with the mass and heat transfer processes in addition to fluid flow. The role of the molecular structure of conjugated molecules in flow-induced crystallization kinetics also requires further investigations. Practically speaking, large-scale application of this technology requires the development of alternative fabrication methods that do not rely on expensive lithographic techniques to direct the printing flow. In summary, we believe that understanding flow-induced morphology evolution is imperative for advancing printed electronics, which will also open up new avenues for attaining high device performance and designing innovative printing technologies.

AUTHOR INFORMATION

Corresponding Author

*E-mail: yingdiao@illinois.edu.

Author Contributions

§G.Q. and J.J.K. contributed equally.

Notes

The authors declare no competing financial interest.

Biographies

Ge Qu received her Bachelor of Chemical Engineering degree from University of Minnesota Twin Cities in 2014. She is pursuing her Ph.D. degree in the Diao group at University of Illinois at Urbana−Champaign from 2014 to present. Her interests include flow-induced alignment, solution printing and interfacial instabilities, advanced X-ray methods for thin film morphology analysis, and device characterizations.

Justin J. Kwok obtained his B.Sc. degree from University of Southern California in 2014. He continued in the Diao group for a Ph.D. degree from 2015 to present. His research focuses on designing innovative printing techniques and understanding nonequilibrium assembly of conjugated polymers.

Ying Diao is the Dow Chemical Company Faculty Scholar and Assistant Professor at University of Illinois at Urbana−Champaign since 2015. She obtained her Ph.D. degree from MIT in 2012 and received postdoctoral training from Prof. Zhenan Bao at Stanford University. Her group at Illinois has been developing fundamental understanding and innovative methodologies for directed assembly of functional materials and their applications in the areas of electronics, renewable energy, and healthcare.

ACKNOWLEDGMENTS

This work was supported by National Science Foundation, Division of Materials Research, under Award ID 1641854.

REFERENCES

(1) Sirringhaus, H. 25th Anniversary Article: Organic Field-Effect Transistors: The Path Beyond Amorphous Silicon. *Adv. Mater.* **2014**, *26*, 1319−1335.

(2) Zhang, Q.; Sun, Y.; Xu, W.; Zhu, D. Organic Thermoelectric Materials: Emerging Green Energy Materials Converting Heat to Electricity Directly and Efficiently. *Adv. Mater.* **2014**, *26*, 6829−6851.

(3) Zhang, C.; Chen, P.; Hu, W. Organic field-effect transistor-based gas sensors. *Chem. Soc. Rev.* **2015**, *44*, 2087−2107.

(4) Sandström, A.; Dam, H. F.; Krebs, F. C.; Edman, L. Ambient fabrication of flexible and large-area organic light-emitting devices using slot-die coating. *Nat. Commun.* **2012**, *3*, 1002.

(5) Diao, Y.; Zhou, Y.; Kurosawa, T.; Shaw, L.; Wang, C.; Park, S.; Guo, Y.; Reinspach, J. A.; Gu, K.; Gu, X.; Tee, B. C.; Pang, C.; Yan, H.; Zhao, D.; Toney, M. F.; Mannsfeld, S. C.; Bao, Z. Flow-enhanced solution printing of all-polymer solar cells. *Nat. Commun.* **2015**, *6*, 7955.

(6) Himmelberger, S.; Salleo, A. Engineering semiconducting polymers for efficient charge transport. *MRS Commun.* **2015**, *5*, 383−395.

(7) Giri, G.; Verploegen, E.; Mannsfeld, S. C.; Atahan-Evrenk, S.; Kim, D. H.; Lee, S. Y.; Becerril, H. A.; Aspuru-Guzik, A.; Toney, M. F.; Bao, Z. Tuning charge transport in solution-sheared organic semiconductors using lattice strain. *Nature* **2011**, *480*, 504−508.

(8) Venkateshvaran, D.; Nikolka, M.; Sadhanala, A.; Lemaur, V.; Zelazny, M.; Kepa, M.; Hurhangee, M.; Kronemeijer, A. J.; Pecunia, V.; Nasrallah, I.; Romanov, I.; Broch, K.; McCulloch, I.; Emin, D.; Olivier, Y.; Cornil, J.; Beljonne, D.; Sirringhaus, H. Approaching disorder-free transport in high-mobility conjugated polymers. *Nature* **2014**, *515*, 384−388.

(9) Diao, Y.; Tee, B. C.; Giri, G.; Xu, J.; Kim, D. H.; Becerril, H. A.; Stoltenberg, R. M.; Lee, T. H.; Xue, G.; Mannsfeld, S. C.; Bao, Z. Solution coating of large-area organic semiconductor thin films with aligned single-crystalline domains. *Nat. Mater.* **2013**, *12*, 665−671.

(10) Xu, J.; Diao, Y.; Zhou, D. S.; Mao, Y. S.; Giri, G.; Chen, W.; Liu, N.; Mannsfeld, S. C. B.; Xue, G.; Bao, Z. N. Probing the interfacial molecular packing in TIPS-pentacene organic semiconductors by surface enhanced Raman scattering. *J. Mater. Chem. C* **2014**, *2*, 2985−2991.

(11) Diao, Y.; Lenn, K. M.; Lee, W.-Y.; Blood-Forsythe, M. A.; Xu, J.; Mao, Y.; Kim, Y.; Reinspach, J. A.; Park, S.; Aspuru-Guzik, A.; Xue, G.; Clancy, P.; Bao, Z.; Mannsfeld, S. C. B. Understanding Polymorphism in Organic Semiconductor Thin Films through Nanoconfinement. *J. Am. Chem. Soc.* **2014**, *136*, 17046−17057.

(12) Chung, H.; Diao, Y. Polymorphism as an emerging design strategy for high performance organic electronics. *J. Mater. Chem. C* **2016**, *4*, 3915.

(13) Noriega, R.; Rivnay, J.; Vandewal, K.; Koch, F. P.; Stingelin, N.; Smith, P.; Toney, M. F.; Salleo, A. A general relationship between disorder, aggregation and charge transport in conjugated polymers. *Nat. Mater.* **2013**, *12*, 1038−1044.

(14) Kleinhenz, N.; Persson, N.; Xue, Z.; Chu, P. H.; Wang, G.; Yuan, Z.; McBride, M. A.; Choi, D.; Grover, M. A.; Reichmanis, E. Ordering of Poly(3-hexylthiophene) in Solutions and Films: Effects of Fiber Length and Grain Boundaries on Anisotropy and Mobility. *Chem. Mater.* **2016**, *28*, 3905−3913.

DOI: 10.1021/acs.accounts.6b00445
Acc. Chem. Res. 2016, 49, 2756−2764

(15) Rivnay, J.; Jimison, L. H.; Northrup, J. E.; Toney, M. F.; Noriega, R.; Lu, S.; Marks, T. J.; Facchetti, A.; Salleo, A. Large modulation of carrier transport by grain-boundary molecular packing and microstructure in organic thin films. *Nat. Mater.* **2009**, *8*, 952−958.
(16) Sirringhaus, H. Device Physics of Solution-Processed Organic Field-Effect Transistors. *Adv. Mater.* **2005**, *17*, 2411−2425.
(17) Diao, Y.; Shaw, L.; Bao, Z.; Mannsfeld, S. C. B. Morphology control strategies for solution-processed organic semiconductor thin films. *Energy Environ. Sci.* **2014**, *7*, 2145−2159.
(18) Mei, J.; Diao, Y.; Appleton, A. L.; Fang, L.; Bao, Z. Integrated Materials Design of Organic Semiconductors for Field-Effect Transistors. *J. Am. Chem. Soc.* **2013**, *135*, 6724−6746.
(19) Treat, N. D.; Nekuda Malik, J. A.; Reid, O.; Yu, L.; Shuttle, C. G.; Rumbles, G.; Hawker, C. J.; Chabinyc, M. L.; Smith, P.; Stingelin, N. Microstructure formation in molecular and polymer semiconductors assisted by nucleation agents. *Nat. Mater.* **2013**, *12*, 628−633.
(20) Schmidt, K.; Tassone, C. J.; Niskala, J. R.; Yiu, A. T.; Lee, O. P.; Weiss, T. M.; Wang, C.; Frechet, J. M.; Beaujuge, P. M.; Toney, M. F. A mechanistic understanding of processing additive-induced efficiency enhancement in bulk heterojunction organic solar cells. *Adv. Mater.* **2014**, *26*, 300−305.
(21) Wang, G.; Persson, N.; Chu, P.-H.; Kleinhenz, N.; Fu, B.; Chang, M.; Deb, N.; Mao, Y.; Wang, H.; Grover, M. A.; Reichmanis, E. Microfluidic Crystal Engineering of π-Conjugated Polymers. *ACS Nano* **2015**, *9*, 8220−8230.
(22) Kwon, S.; Yu, K.; Kweon, K.; Kim, G.; Kim, J.; Kim, H.; Jo, Y.-R.; Kim, B.-J.; Kim, J.; Lee, S. H.; Lee, K. Template-mediated nanocrystallite networks in semiconducting polymers. *Nat. Commun.* **2014**, *5*, 4183.
(23) Kang, B.; Jang, M.; Chung, Y.; Kim, H.; Kwak, S. K.; Oh, J. H.; Cho, K. Enhancing 2D growth of organic semiconductor thin films with macroporous structures via a small-molecule heterointerface. *Nat. Commun.* **2014**, *5*, 4752.
(24) Tseng, H. R.; Ying, L.; Hsu, B. B.; Perez, L. A.; Takacs, C. J.; Bazan, G. C.; Heeger, A. J. High mobility field effect transistors based on macroscopically oriented regioregular copolymers. *Nano Lett.* **2012**, *12*, 6353−6357.
(25) Minemawari, H.; Yamada, T.; Matsui, H.; Tsutsumi, J.; Haas, S.; Chiba, R.; Kumai, R.; Hasegawa, T. Inkjet printing of single-crystal films. *Nature* **2011**, *475*, 364−367.
(26) Goto, O.; Tomiya, S.; Murakami, Y.; Shinozaki, A.; Toda, A.; Kasahara, J.; Hobara, D. Organic single-crystal arrays from solution-phase growth using micropattern with nucleation control region. *Adv. Mater.* **2012**, *24*, 1117−1122.
(27) Diao, Y.; Harada, T.; Myerson, A. S.; Hatton, T. A.; Trout, B. L. The role of nanopore shape in surface-induced crystallization. *Nat. Mater.* **2011**, *10*, 867−871.
(28) Schott, S.; Gann, E.; Thomsen, L.; Jung, S. H.; Lee, J. K.; McNeill, C. R.; Sirringhaus, H. Charge-Transport Anisotropy in a Uniaxially Aligned Diketopyrrolopyrrole-Based Copolymer. *Adv. Mater.* **2015**, *27*, 7356−7364.
(29) Bucella, S. G.; Luzio, A.; Gann, E.; Thomsen, L.; McNeill, C. R.; Pace, G.; Perinot, A.; Chen, Z.; Facchetti, A.; Caironi, M. Macroscopic and high-throughput printing of aligned nanostructured polymer semiconductors for MHz large-area electronics. *Nat. Commun.* **2015**, *6*, 8394.
(30) Becerril, H. A.; Roberts, M. E.; Liu, Z.; Locklin, J.; Bao, Z. High-Performance Organic Thin-Film Transistors through Solution-Sheared Deposition of Small-Molecule Organic Semiconductors. *Adv. Mater.* **2008**, *20*, 2588−2594.
(31) Park, H. J.; Kang, M. G.; Ahn, S. H.; Guo, L. J. A facile route to polymer solar cells with optimum morphology readily applicable to a roll-to-roll process without sacrificing high device performances. *Adv. Mater.* **2010**, *22*, E247−253.
(32) Krebs, F. C. Fabrication and processing of polymer solar cells: A review of printing and coating techniques. *Sol. Energy Mater. Sol. Cells* **2009**, *93*, 394−412.
(33) Søndergaard, R. R.; Hösel, M.; Krebs, F. C. Roll-to-Roll fabrication of large area functional organic materials. *J. Polym. Sci., Part B: Polym. Phys.* **2013**, *51*, 16−34.
(34) Mullin, J. W.; Raven, K. D. Nucleation in Agitated Solutions. *Nature* **1961**, *190*, 251−251.
(35) Mullin, J. W.; Raven, K. D. Influence of Mechanical Agitation on the Nucleation of Some Aqueous Salt Solutions. *Nature* **1962**, *195*, 35−38.
(36) Yang, H.; Yu, X.; Raval, V.; Makkawi, Y.; Florence, A. Effect of Oscillatory Flow on Nucleation Kinetics of Butyl Paraben. *Cryst. Growth Des.* **2016**, *16*, 875−886.
(37) Le Berre, M.; Chen, Y.; Baigl, D. From convective assembly to Landau-Levich deposition of multilayered phospholipid films of controlled thickness. *Langmuir* **2009**, *25*, 2554−2557.
(38) Deegan, R. D.; Bakajin, O.; Dupont, T. F.; Huber, G.; Nagel, S. R.; Witten, T. A. Capillary flow as the cause of ring stains from dried liquid drops. *Nature* **1997**, *389*, 827−829.
(39) Giri, G.; Li, R.; Smilgies, D.-M.; Li, E. Q.; Diao, Y.; Lenn, K. M.; Chiu, M.; Lin, D. W.; Allen, R.; Reinspach, J.; Mannsfeld, S. C. B.; Thoroddsen, S. T.; Clancy, P.; Bao, Z.; Amassian, A. One-dimensional self-confinement promotes polymorph selection in large-area organic semiconductor thin films. *Nat. Commun.* **2014**, *5*, 3573.
(40) Park, S.; Giri, G.; Shaw, L.; Pitner, G.; Ha, J.; Koo, J. H.; Gu, X.; Park, J.; Lee, T. H.; Nam, J. H.; Hong, Y.; Bao, Z. Large-area formation of self-aligned crystalline domains of organic semiconductors on transistor channels using CONNECT. *Proc. Natl. Acad. Sci. U. S. A.* **2015**, *112*, 5561−5566.
(41) Mullins, W. W.; Sekerka, R. F. Stability of a Planar Interface During Solidification of a Dilute Binary Alloy. *J. Appl. Phys.* **1964**, *35*, 444−451.
(42) Mullins, W. W.; Sekerka, R. F. Morphological Stability of a Particle Growing by Diffusion or Heat Flow. *J. Appl. Phys.* **1963**, *34*, 323−329.
(43) Mullin, J. W. *Crystallization*, 4th ed.; Butterworth-Heinemann: Oxford; Boston, MA, 2001.
(44) Langer, J. S. Instabilities and pattern formation in crystal growth. *Rev. Mod. Phys.* **1980**, *52*, 1−28.
(45) Tartakovsky, A. M.; Meakin, P.; Scheibe, T. D.; Eichler West, R. M. Simulations of reactive transport and precipitation with smoothed particle hydrodynamics. *J. Comput. Phys.* **2007**, *222*, 654−672.
(46) Wang, Y.; Chen, L.; Wang, Q.; Sun, H.; Wang, X.; Hu, Z.; Li, Y.; Shi, Y. Solution-processed organic crystals written directly with a rollerball pen for field-effect transistors. *Org. Electron.* **2014**, *15*, 2234−2239.
(47) Reiter, G. Some unique features of polymer crystallisation. *Chem. Soc. Rev.* **2014**, *43*, 2055−2065.
(48) Miura, T.; Kishi, R.; Mikami, M.; Tanabe, Y. Effect of rigidity on the crystallization processes of short polymer melts. *Phys. Rev. E: Stat. Phys., Plasmas, Fluids, Relat. Interdiscip. Top.* **2001**, *63*, 061807.
(49) Lamberti, G. Flow induced crystallisation of polymers. *Chem. Soc. Rev.* **2014**, *43*, 2240−2252.
(50) Lagasse, R. R.; Maxwell, B. An experimental study of the kinetics of polymer crystallization during shear flow. *Polym. Eng. Sci.* **1976**, *16*, 189−199.
(51) Pennings, A. J.; Kiel, A. M. Fractionation of polymers by crystallization from solution, III. On the morphology of fibrillar polyethylene crystals grown in solution. *Colloid Polym. Sci.* **1965**, *205*, 160−162.
(52) Wang, G.; Chu, P. H.; Fu, B.; He, Z.; Kleinhenz, N.; Yuan, Z.; Mao, Y.; Wang, H.; Reichmanis, E. Conjugated Polymer Alignment: Synergisms Derived from Microfluidic Shear Design and UV Irradiation. *ACS Appl. Mater. Interfaces* **2016**, *8*, 24761−24772.
(53) Wie, J. J.; Nguyen, N. A.; Cwalina, C. D.; Liu, J.; Martin, D. C.; Mackay, M. E. Shear-Induced Solution Crystallization of Poly(3-hexylthiophene) (P3HT). *Macromolecules* **2014**, *47*, 3343−3349.

DOI: 10.1021/acs.accounts.6b00445
Acc. Chem. Res. 2016, 49, 2756−2764